Load capability estimation of dry-type transformers used in PV-systems by employing field measurements

Alvarez, David; Restrepo, Jorge; Silva, Filipe Miguel Faria da; Rosero, Javier

Published in:
Electrical Engineering

DOI (link to publication from Publisher):
10.1007/s00202-020-01148-7

Publication date:
2021

Document Version
Accepted author manuscript, peer reviewed version

Noname manuscript No.
(will be inserted by the editor)

Load Capability Estimation of Dry-Type Transformers Used in PV-Systems by Employing Field Measurements

David L. Alvarez · Jorge Restrepo · F. Faria da Silva · Javier Rosero

Received: date / Accepted: date

Abstract Transformer insulation aging is a critical issue for both reliable and economic operations, and for planning of electrical systems. As insulation aging depends on the hottest-spot temperature, transformer management can be improved with a suitable model for temperature estimation and prediction. However, the temperature inside transformers varies dynamically because of changes in both the cooling conditions and the load cycles. Hence, this paper presents an algorithm to estimate and predict the hottest-spot in Dry-Type distribution transformers, so that their capability and insulation life can be assessed. This procedure is focused on transformers used to directly connect PV-inverters to the grid in order to consider the uncontrolled power generation of distribution PV-systems. To implement the algorithm, it is assumed that records of ambient temperature, PV-system power generation cycle, and winding temperature are available. With this data, the parameters of an equivalent thermal circuit are fitted in order to dynamically model the transformer hottest-spot. The method was validated using twelve-day records of a 70 kW_p PV-generation system connected to a 75 kVA Dry-Type transformer. Results show that an enhancement in the hot-spot estimation is reached, and an assessment of the performance in real-time monitoring of the transformer capacity is achieved employing the proposed algorithm.

Keywords Dry-Type Transformer, Dynamic Thermal Rating, Extended Kalman Filter, State Estimation, Thermal transient

1 Introduction

Photovoltaic (PV) generation at the distribution level has increased in recent years. These generation systems are usually located on the rooftops of houses or other

David L. Alvarez · Jorge Restrepo · Javier Rosero
Department of Electrical and Electronic Engineering, Universidad Nacional de Colombia
Cra. 30 No 45-03, Edificio 453 – 208, Bogotá, Colombia
E-mail: dlalvareza@unal.edu.co

F. Faria da Silva
Department of Energy Technology, Aalborg University, Aalborg, Denmark
E-mail: ffs@et.aau.dk

buildings. When the output voltage of the PV-system inverter is different from grid voltage, it is necessary to use transformers. Due to space restrictions in buildings, as well as security requirements, Dry-Type transformers are frequently used for distributed PV-generation.

One characteristic of PV-generation is its intermittent power injection. To reduce this impact, energy storage can be used. However, this technology still faces economic challenges for implementation at the distribution level, and so PV-systems are often connected directly to the grid through a transformer. In those transformers, the load varies continuously and so does the hottest-spot temperature, as a consequence of the uncontrolled power injection. This temperature presents a transient behavior, which depends on the initial thermal conditions and the transformer cooling characteristics, as well as on power production and external weather, among others [17]. All those factors influence the insulation life expectancy.

Transformer life expectancy is related to insulation aging, which is deteriorated by the hottest-spot temperature [8]. This hot-spot is a function of the losses produced by Joule effect and therefore depends on the transformer loading. Hence, transformer thermal capability is defined by the hottest-spot guarantying its life expectancy. The effects of harmonics in transformer life expectancy as a result of PV-systems with direct connection to the grid are analyzed in [3]; in the paper, it is assumed that the transformer operates at rated load and under thermal steady state (worst case loading scenario). This means that the dynamic behavior of the power production, the ambient temperature, and the thermal transient are not considered. According to [16], when incorporating distributed PV-generation at the distribution level for self consumption, the transformer insulation life expectancy is extended because the daily load curve of the transformer decreases and so does its insulation thermal stress. This occurs mainly because in summer, when maximum load peak takes place, the self consumption PV-system is expected to produce maximum power, resulting in a transformer load decrease and consequently in a reduction of the insulation thermal stress.

PV-systems generation depends on solar radiation, which itself varies along the day. At night, a decrease in the transformer temperature is expected until it reaches a stable state. This phenomenon takes place because the generation is null and only no-load losses occur. Subsequently, the transformer temperature begins to rise with the sunrise in a dynamic way [7]. During this thermal transient, the hottest-spot value can increase or decrease as a consequence of the variations of both ambient temperature and load. With these variations, the transformer probably reaches the maximum rated hottest-spot only during few periods of time, or does not reach it at all.

Commonly, power and distribution transformers are designed for a rated load, assuming certain conservative conditions such as the maximum and average ambient temperature, a constant load, specific cooling conditions, altitude of operation, operation at thermal steady state, among others. The fulfilment of those conditions ensures a transformer reaches its normal life expectancy [8]. However, these can vary during transformer operations. Hence, by knowing or monitoring these conditions, together with an accurate dynamic model by which transient thermal phenomena are described, it is possible to predict transformer load capability [5]. Such strategy allow enhancing transformer operation and planning [10], without sacrificing the asset life expectancy [23]. For instance, IEEE Std C57.159$^{\text{TM}}$-2016

[7] suggests considering the rate of the PV-transformer based on the load profile. In [13,11] the numerical methods Finite Element Analysis (FEA) and Computational Fluid Dynamics (CFD) were used to model the temperature distribution in dry-type transformers. In [4], overloads in dry-type transformers were assessed running multiple CFD simulations in order to obtain relations between the hottest-spot, time, and load; each simulation lasted 3 h. Therefore, CFD is not suitable for real-time thermal monitoring and assessment, because it demands a lot of computational resources and processing time. For this reason, in oil-immersed transformers, both the top-oil and the hottest-spot temperature are modeled by equivalent thermal circuits [20]. These types of thermal circuits are used to dynamically assess load capability of transformers [14]. However, these equivalent circuits depend on constant values, which are assumed or given by standards, resulting in inaccuracies in transformer dynamic thermal modeling. In order to reduce those inaccuracies, experimental tests can be employed to obtain thermal constants. For instance, in [24], an algorithm to estimate the oil exponent of traction transformers is proposed. In [21], both thermal oil exponent and time constant are estimated using a non-linear integral-squared error objective function.

This paper proposes a methodology to assess load capability of Dry-Type transformers using estimations of hot-spot temperature. The methodology uses an equivalent thermal circuit and assumes that the values of solar radiation or PV-generation and ambient temperature are provided, either via measurements or from weather forecast models. The temperature is estimated by an Extended Kalman Filter (EKF) using field measurements; the procedure proposed in [1] for oil immersed transformers is followed. Using the EKF, the core temperature and the hottest-spot are estimated, and the parameters of the assumed equivalent thermal circuit fitted. With this methodology, the decision making can be supported during transformer operation and planning, in particular for PV-generation systems. For instance, transformer design criteria can be changed using radiation and ambient temperature, PV-generation systems with more panels can be linked to a same transformer, transformer overloading can be managed in order to reduce the load shedding, among others. Finally, the proposed methodology can be used for dynamic thermal rating.

2 Dry-Type Transformer Thermal Model

According to IEEE Std C57.96$^{\mathrm{TM}}$-2013 [8], thermal transients in dry-type transformers can be modeled by a differential equation. This equation is a function of the losses, the thermal conditions prior to the transient and the transformer cooling characteristics. The transformer cooling depends on both the geometry and the material physical parameters. Using this standard and a transformer equivalent thermal circuit, as proposed by Susa [20], the simplified thermal circuit shown in fig. 1 can be used, where Θ_{HS} is the hottest-spot winding temperature, Θ_a is the ambient temperature, $\Delta\Theta_{HS} = \Theta_{HS} - \Theta_a$ is the hottest-spot temperature rise above ambient temperature, and R is the equivalent non-linear thermal resistance of the entire transformer [19]. This resistance depends on the transformer operating temperature and its characteristics, including cooling type. At rating conditions, the resistance can be estimated using transformer nameplate or tem-

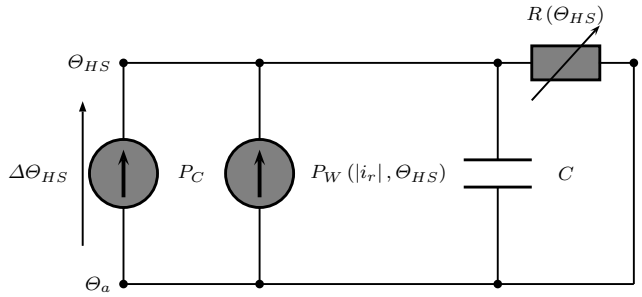

Fig. 1: Equivalent thermal circuit used to model the dynamic behaviour of transformer temperature

perature rise test. Finally, C is the effective thermal capacity of the winding and core.

The hottest-spot of the circuit shown in fig. 1 is determined by:

$$\frac{d\Theta_{HS}}{dt} = \frac{P_C + P_W\left(|i_r|, \Theta_{HS}\right) - \dfrac{\Delta\Theta_{HS}}{R\left(\Theta_{HS}\right)}}{C} \tag{1}$$

where P_C are the core losses or no-load losses and $P_W\left(|i_r|, \Theta_{HS}\right)$ are the winding losses, also known as the load losses. $P_W\left(|i_r|, \Theta_{HS}\right)$ varies with the average temperature of the conductor and with the current intensity that flows through the windings ($|i_r|$). Commonly, this current intensity is expressed in terms of the load. The variation of the electrical resistance, and therefore of the load losses, as a function of the hottest-spot can be approximated by the following equation:

$$P_W = L^2\left(P_{i^2R,R}K_T + \frac{P_{eddy,R}}{K_T}\right) \tag{2}$$

where L is the per-unit load; $P_{i^2R,R}$ and $P_{eddy,R}$ refer to DC losses and eddy losses in the windings (load-losses) at rated load condition and known reference temperature, respectively. P_{eddy} can be estimated using factory test, and corresponds to the difference between load and DC resistance losses. K_T is the temperature correction factor, that takes into account resistance variation with temperature. This factor is approximated by:

$$K_T = \frac{T_k + \Theta_{HS}}{T_k + \Theta_{ref}} \tag{3}$$

where T_k is the conductor temperature constant [8] (225 for aluminum and 234.5 for copper) and Θ_{ref} is the losses reference temperature. Voltage harmonics as well as current also have an impact on core and winding temperatures. In IEEE Std C.57.110-2010 [12], this impact is modeled by an increase in both i^2R losses and eddy losses. The thermal performance of the PV transformer operating under reverse power flow will depend on the same conditions that in normal operation, such as the current magnitude, harmonic content, voltage value, etc, and thus can be modeled by eq. (1).

According to eq. (1), thermal resistance varies as a consequence of the temperature dependence of cooling properties. This thermal resistance is a black box model of the cooling properties, describing the heat transfer by conduction, convection and radiation. For power transformers immersed in oil, the variable with the highest influence on the cooling regarding the temperature is the oil viscosity [20]. Nevertheless, according to [4], in dry-type transformers, the variable with the highest influence on the cooling in relation with the temperature is the air density. Based on the modeling of transformers immersed in oil, this paper proposes modeling the influence of temperature on the air physical parameters in terms of an equivalent thermal resistance by through the following equation:

$$R\left(\Theta_{HS}\right) = R_{0,R}\left(\frac{\rho\left(\Theta_{HS}\right)}{\rho\left(\Theta_{HS,R}\right)}\right)^{m} \tag{4}$$

where $\rho\left(\Theta_{HS}\right)$ and $\rho\left(\Theta_{HS,R}\right)$ are the air density at current temperature and at rated conditions, respectively, and m is an empirical constant, which describes the behavior of the thermal resistance as a function of the temperature. In this paper, m is assumed unknown and constitutes therefore a parameter to be estimated. $R_{0,R}$ is the thermal resistance at rated condition given by:

$$R_{0,R} = \frac{\Delta\Theta_{HS,R}}{P_R} \tag{5}$$

where $\Delta\Theta_{HS,R}$ is the rated hottest-spot temperature rise over ambient and P_R are the transformer losses at rated load. In [4], the influence of temperature in the air density is approximated as follows:

$$\rho\left(\Theta_{HS}\right) = 2.711 - 0.006711 \cdot \Theta_{HS} + 5.364 \times 10^{-6} \cdot {\Theta_{HS}}^{2} \tag{6}$$

where Θ_{HS} must be in K.

Finally, the effective thermal capacity (C) depends on the materials physical parameters as well as on their masses. This parameter can be estimated as the sum of all materials masses multiplied by their specific heat according to IEEE Std C57.96™-2013 [8], as follows:

$$C = \frac{m_p C_p}{n} = \frac{m_{core}C_{core} + m_{wind.}C_{wind.} + m_{ins.}C_{ins.}}{n} \tag{7}$$

where m_p and C_p are the equivalent mass and specific heat of the entire transformer, which includes the core (m_{core}, C_{core}), the windings ($m_{wind.}, C_{wind.}$), and the insulation ($m_{ins.}, C_{ins.}$). Transformers are manufactured with different materials such as copper, aluminum, magnetic sheets, insulating materials, among others, but their respective masses are usually unknown by owners and operators. Therefore, this work proposes using a constant n to represent the thermal capacitance uncertainty, as a consequence of unknown values in both the masses and specific heat of the transformer materials. That constant must be evaluated within the model using measurements. The procedure is addressed in the below section.

3 Proposed Procedure

This section presents the algorithm proposed to estimate the load capability of Dry-Type transformers used in PV-generation systems. The algorithm is based on an Extended Kalman Filter (EKF) [18]. To implement the algorithm, both the transformer nameplate and measurements of ambient temperature, hot-spot and loading should be provided. As the assumed dynamic thermal model is non linear, EKF was chosen instead of the standard Kalman Filter (KF). The performance of EKF to estimate and predict thermal states in power systems assets was addressed previously in [1,9,2].

In short, EKF algorithms are based on the estimation of the current state as well as in the minimization of the error covariance of a dynamic system. Figure 2 shows a graph explanation of the EKF: an initial estimation $\left(\hat{x}_{k-1}^{+}\right)$ of the dynamic system state is assumed, and this system is modeled by a differential equation. With this initial value and with the dynamic model of the system, a state prediction $\left(\hat{x}_{k}^{-}\right)$ can be computed from instant t_{k-1} to instant t_k. This prediction depends on the control variables, which are assumed to be known. However, during the prediction, an error propagation occurs as a consequence of errors in: the initial estimated value $\left(\hat{x}_{k-1}^{+}\right)$, the control variables and the model of the system. The uncertainty in the error propagation can be modeled by the covariance $\left(\hat{P}_{k}^{-}\right)$, which is computed with the EKF. Next, a set of measurements ($\mathbf{z}$) of the system at instant t is used to update both the estimation $\left(\hat{x}_{k}^{+}\right)$ and the error covariance $\left(\hat{P}_{k}^{+}\right)$. This procedure is repeated for each new measurement set.

Equation (1) is used to model the dynamic system. The hottest-spot (Θ_{HS}) and the constants m and n of eqs. (4) and (7) are defined as the state variables ($\mathbf{x}$) given the uncertainties on these values $\left(\mathbf{x} = \left[\Theta_{HS}\ m\ n\right]^{\top}\right)$. That, taking advantage of the EKF capacity to fit constants [18]. As control variables ($\mathbf{u}$), the PV-generation (L) and the ambient temperature (Θ_a) are considered $\left(\mathbf{u} = \left[L\ \Theta_a\right]\right)$. Finally, discrete measurements of temperature ($\mathbf{z}$) at the assumed windings hottest-spot and/or at the core $\left(\mathbf{z}_k = \left[\Theta_{HS_k} + \mathbf{v}_k\right]\right)$ are made, with $\mathbf{v}$ being the measurement noise. The equations developed by the authors used to implement the algorithm can in found in the appendix section. Using this set of equations, it is proposed to model, estimate and predict the load capability of a PV-transformer using an EKF. A summary of the algorithm here employed is presented in fig. 3.

4 Algorithm Validation Results

To assess the performance of the algorithm, field measurements were used to evaluate the algorithm, seeking to estimate the load capability of a dry-type transformer and, therefore, to validate the proposed procedure.

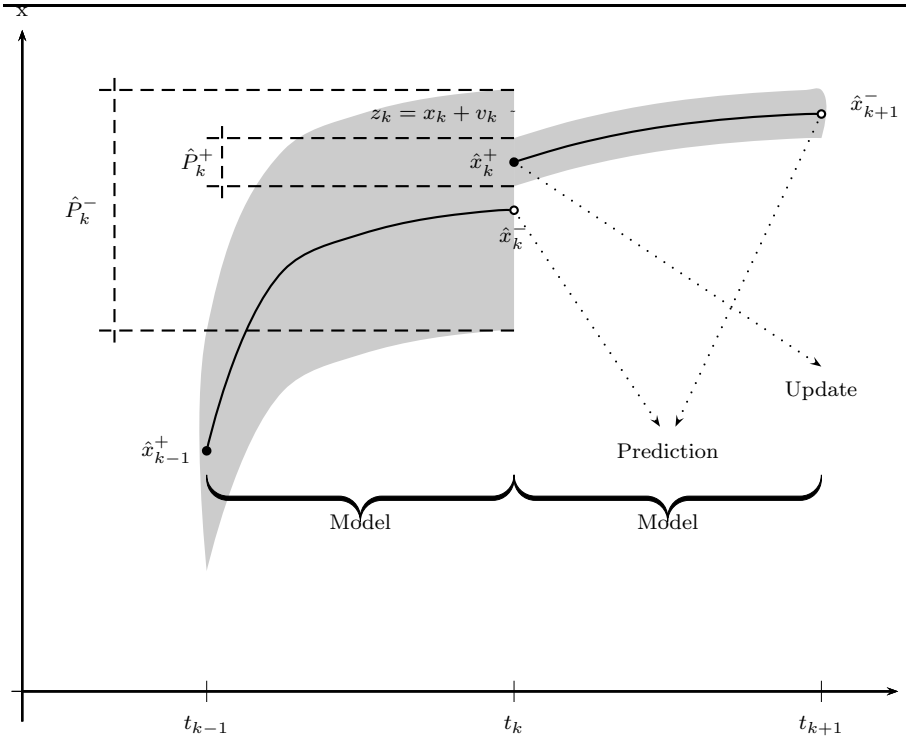

Fig. 2: Graphical explanation of the implemented Extended Kalman Filter

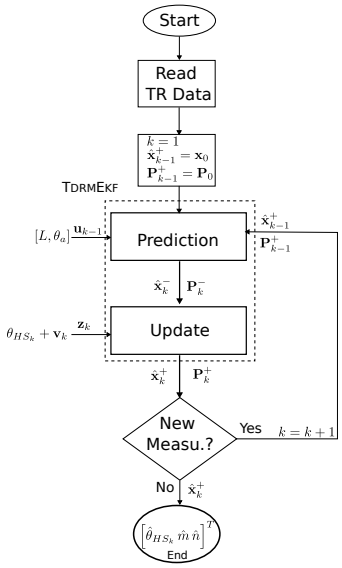

(a) Procedure Flowchart

1: **procedure** TDRMEKF($\mathbf{z}_k$,$\mathbf{u}_k$,$\hat{\mathbf{x}}_{k-1}^+$,$\mathbf{P}_{k-1}^+$,δt,t_k,$\mathbf{Q}$,$\mathbf{R}_k$) ▷ δt, $\mathbf{Q}$, $\mathbf{R}_k$ are the time step, the model error covariance and the measurements error covariance, respectively
2: $\hat{\mathbf{x}}_k^- \leftarrow \hat{\mathbf{x}}_{k-1}^+$ ▷ State variables
3: $\mathbf{P}_k^- \leftarrow \mathbf{P}_{k-1}^+$ ▷ Covariance error
4: **for** $j \leftarrow \delta_t$ **to** t_k **step** δ_t **do** ▷ Prediction
5: $\dot{\hat{\mathbf{x}}}_k^- \leftarrow \mathbf{f}\left(\hat{\mathbf{x}}_k^-, \mathbf{u}_k, 0, \delta_t\right)$ ▷ Model, eq. (8)
6: $\hat{\mathbf{x}}_k^- \leftarrow \hat{\mathbf{x}}_k^- + \dot{\hat{\mathbf{x}}}_k^-$
7: $\mathbf{F} \leftarrow \partial \mathbf{f}/\partial \mathbf{x}|_{\hat{\mathbf{x}}_k^-, \mathbf{u}_k}$ ▷ eqs. (9) to (11)
8: $\mathbf{L} \leftarrow \partial \mathbf{f}/\partial \mathbf{w}|_{\hat{\mathbf{x}}_k^-, \mathbf{u}_k}$ ▷ eqs. (12) and (13)
9: $\dot{\mathbf{P}}_k^- \leftarrow \mathbf{F}\mathbf{P}_k^- + \mathbf{P}_k^-\mathbf{F}^T + \mathbf{L}\mathbf{Q}\mathbf{L}^T$
10: $\mathbf{P}_k^- \leftarrow \mathbf{P}_k^- + \dot{\mathbf{P}}_k^-$
11: **end for**
12: $\mathbf{H}_k \leftarrow \partial \mathbf{h}/\partial \mathbf{x}|_{\hat{\mathbf{x}}_k^-}$
13: $\mathbf{M}_k \leftarrow \partial \mathbf{h}/\partial \mathbf{v}|_{\hat{\mathbf{x}}_k^-}$
14: $\mathbf{K}_k \leftarrow \mathbf{P}_k^-\mathbf{H}_k^T\left(\mathbf{H}_k\mathbf{P}_k^-\mathbf{H}_k^T + \mathbf{M}_k\mathbf{R}_k\mathbf{M}_k^T\right)^{-1}$
15: $\hat{\mathbf{x}}_k^+ \leftarrow \hat{\mathbf{x}}_k^- + \mathbf{K}_k\left(\mathbf{z_k} - \mathbf{h}\left(\hat{\mathbf{x}}_k^-\right)\right)$ ▷ Update state variables
16: $\mathbf{P}_k^+ \leftarrow \left(\mathbf{I} - \mathbf{K}_k\mathbf{H}_k\right)\mathbf{P}_k^-\left(\mathbf{I} - \mathbf{K}_k\mathbf{H}_k\right)^T + \mathbf{K}_k\mathbf{M}_k\mathbf{R}_k\mathbf{M}_k^T\mathbf{K}_k^T$ ▷ Update covariance error
17: **return** $\left(\hat{\mathbf{x}}_k^+, \mathbf{P}_k^+\right)$
18: **end procedure**

(b) EKF pseudo code

Fig. 3: Proposed loading capability estimation algorithm

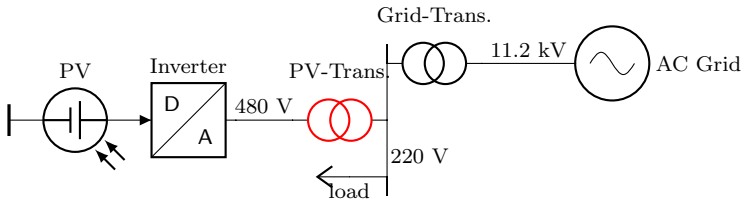

Fig. 4: PV-System used to validate the proposed EKF algorithm

Table 1: Dry-Type Transformer's Parameters and Characteristics

Parameter	Value	Units
S	75	kV A
$\Delta\Theta_{HS,R}$	180	K
Θ_a	30	°C
P_C	372	W
Θ_{ref}	25	°C
P_{i^2R}	1003	W
P_E	16	W
m_p	310	kg
C_p	15×60	$\mathrm{J\,kg^{-1}\,K}$
Class	H	
Winding's Material	Al	
Cooling class	AN	

4.1 Case Study

Figure 4 shows the PV-system used to validate the proposed algorithm. This system is composed of 70 $\mathrm{kW_p}$ PV-generation panels, a 60 kW inverter, and a 75 kVA-480/220 V three phase class H dry-type transformer (PV-Trans), also known as inverter transformer [7]. The transformer cooling class is ventilated self-cooled (AN). The inverter power rating is less than the maximum power output expected from the panels, because during the financial evaluation this was the most cost/effective decision. In other words, the expected energy gain deriving from the use of a higher rated inverter did not compensate the additional cost of the inverter [15]. The PV-system is located at the rooftop of the Medicine building of the Universidad Nacional de Colombia in Bogota. The transformer outputs are connected to the building's bus feeder as shown in the diagram. The power generated mainly feeds the self-consumption of the building.

Table 1 shows the PV-transformer thermal parameters and properties. This data was obtained from the nameplate and factory test-report.

In order to implement the algorithm, measurements of temperature and load were made in the PV-System. Figure 5 shows the use of PT-100 probes (thermoresistive sensors) to measure the ambient temperature, the assumed hottest-spot temperature of the inner winding and the core temperature (center leg). Temperature probes locations were chosen taking into account IEEE Std C57.134 [6] recommendations. A power meter was used to measure the total power that flowed through the transformer. This information was monitored in real time and stored using the platform lab+i [22]. The sample rate was 5 min.

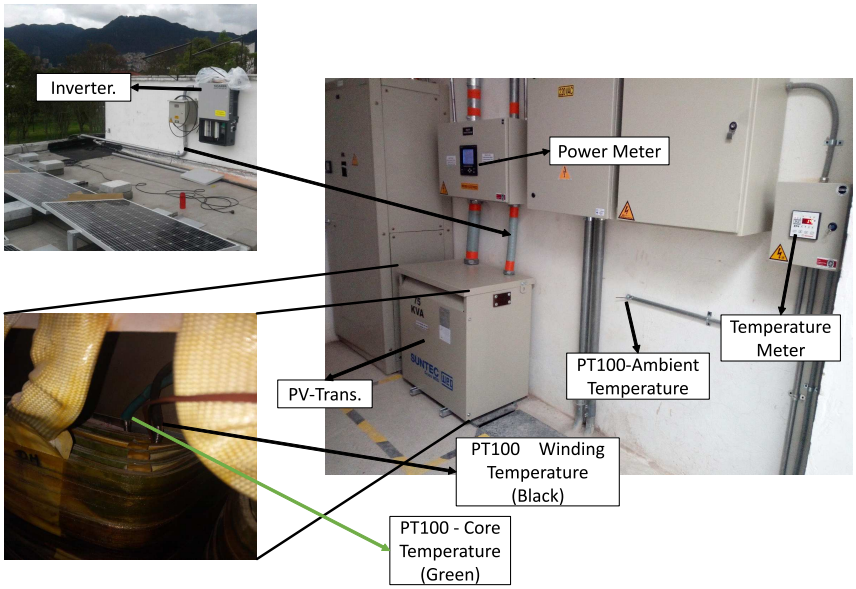

Fig. 5: PV-generation system setup

The proposed EKF algorithm was implemented by using MATLAB®. Equation (1) was solved through numerical integration with time steps of $\delta_t = 30\,\mathrm{s}$. Covariance errors of $diag\,(\mathbf{Q}) = \left[Q_s = 10^{-7}\,\mathrm{K}^2\ Q_L = (0.001/3)^2\ Q_{\theta_a} = (1/3)^2\,\mathrm{K}^2\right]$ and $R_k = (1/3)^2\ \mathrm{K}^2$ for the control variables and hottest-spot/core temperatures were used, respectively. Initial values of the constants were fixed to $n_0 = 1$ and $m_0 = 1$. To set the algorithm, a 12-day measurement window was used.

4.2 Temperature and Parameters Estimation

Figures 6 and 7 show the measurements of ambient temperature (Θ_A), hottest-spot (Θ_{HS}), load (L), and the temperatures estimated with the proposed EKF at the hottest-spot $\left(\hat{\Theta}_{HS}\right)$ and core. The ambient temperature was measured with a PT-100 probe as shown in fig. 5. According to the measured profile, the ambient temperature varies less than 2 K during an entire day, because the transformer is located indoors and in a tropical zone. As a result of EKF usage, the root mean square residuals (ϵ) obtained between estimations and measurements were 1.2 K for the hottest-spot and 0.81 K for the temperature of the core.

Figure 8 shows the fitting of the parameters n and m for the hottest-spot ($n = 4, m = 0.89$) and core temperature ($n = 1.3, m = 1.88$), respectively. These parameters were estimated using the previous measurements and the proposed EKF. Both values of n and m converged to constant values, as expected. The differences between these constants are a consequence of the different thermal parameters in the heat transfer between the windings and the core. Finally, according to IEEE Std C57.96™ [8], if the transformer had a different cooling class, such as ventilated forced-air-cooled (AF), the value of thermal exponent constant would

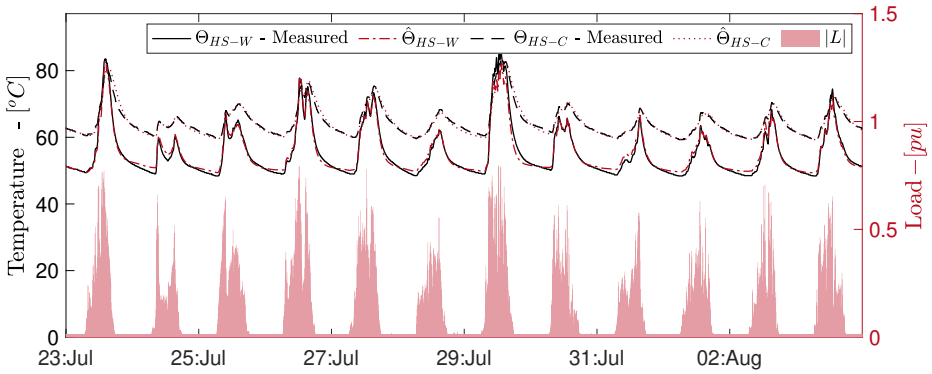

Fig. 6: Evolution of measured and estimated hottest-spot ($\Theta_{HS-W} - Measured$), $\left(\hat{\Theta}_{HS-W}\right)$, and core temperature ($\Theta_{HS-C} - Measured$) and $\left(\hat{\Theta}_{HS-C}\right)$ with time, in accordance with load variation ($|L|$)

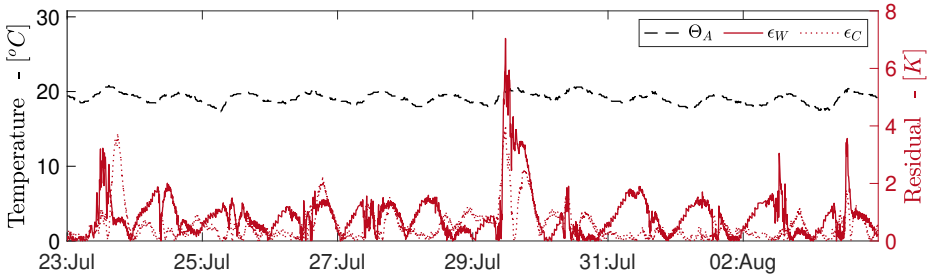

Fig. 7: Ambient temperature (Θ_A), and residual (ϵ) between measurements and estimations

be different. However, this issue must be validated using the proposed EKF in future research.

4.3 Performance Comparison

To assess the performance of the algorithm, the proposed procedure is compared with recommendations for loading dry-type distribution and power transformers given by IEEE Std C57.96™-2013 [8]. The results are shown in fig. 9, where the hottest-spot winding temperature measured, estimated with the EKF and calculated using the C57.96™-2013 recommendations are plotted. The root mean square error obtained between the measurements and the IEEE Std. was $\epsilon \approx 5.8\,\mathrm{K}$ which is greater than $\epsilon \approx 1.2\,\mathrm{K}$ obtained using the proposed procedure.

Computing the hottest-spot winding temperature with the IEEE Std thanks to the suggest empirical exponent constant $m = 0.8$, an error $\epsilon \approx 23\,\mathrm{K}$ was obtained. However, according to this standard, it is possible to use a different value of m if it can be justified by test data. Hence, to reduce this error, combinatorial method was used to fit both m to 0.53, and the thermal capacitance. Multiplying this last

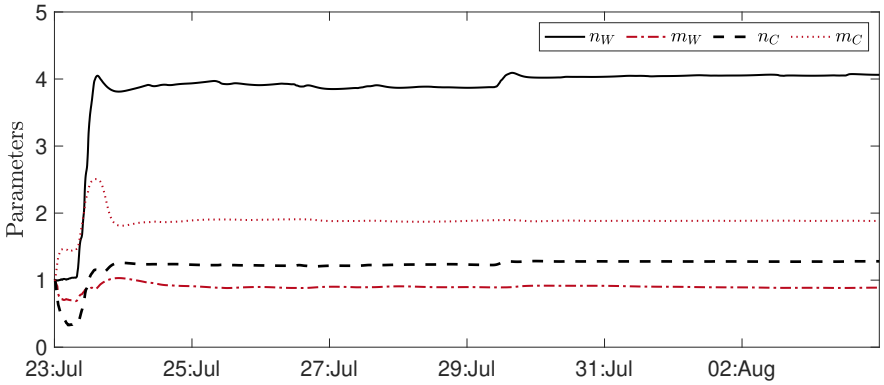

Fig. 8: Estimation of n and m parameters using the proposed algorithm, for hottest-spot and core temperature

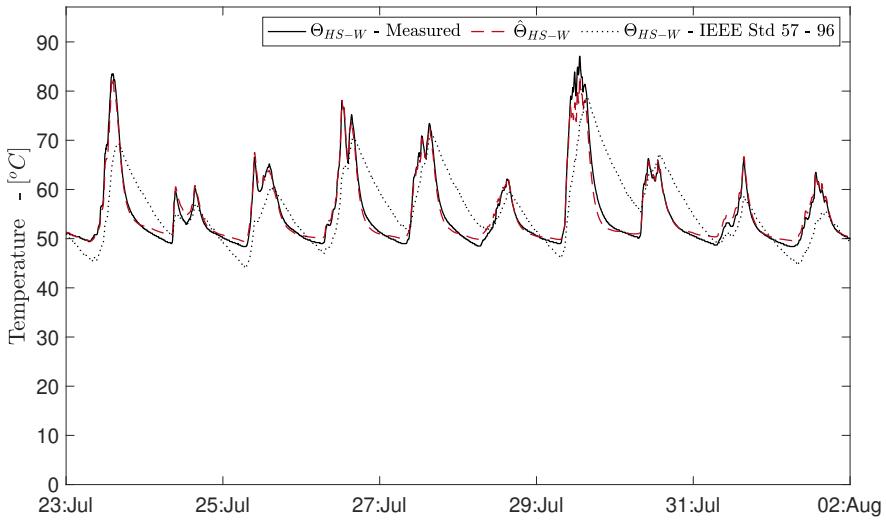

Fig. 9: Comparison of hottest-spot measurements ($\Theta_{HS-W} - Measured$), and estimation using the proposed model $\left(\hat{\Theta}_{HS-W}\right)$ and IEEE Std C57.96™-2013 recommendations (Θ_{HS-W} – IEEE Std 57 - 96)

parameter by a constant of 1.27, a minimum error of $\epsilon \approx 5.8$ Kwas obtained for this case. The differences between the exponent m suggested by the IEEE Std and the value fitted by the authors can be associated to the indoor area, the tank wall that influences the natural ventilation, and the altitude of the transformer under study respecting to standard conditions described in C57.96™-2013.

4.4 Load Capability Estimation

According to the results obtained in the previous section, the maximum temperature inside the transformer was 87 °C at the winding. Under these PV-generation conditions, the transformer can be overloaded, since for Dry-type transformers, the rated hottest-spot must be 10 K lower than the temperature class [8]: in this case 180 °C for class H transformers. Hence, in order to estimate the maximum allowed output power, the generation profile measured was extrapolated increasing the power generation until the computed hottest-spot reached the maximum allowed temperature in the insulation. This temperature was computed using eq. (1) and the estimated constants m and n. As a result, the maximum allowed generation estimated was 1.95 times the current generation. In other words, according to the dynamic simulation, the 75 kVA transformer could stand approximately 140 kW of PV-generation under the assumed conditions, without affecting the insulation life expectancy. For outdoor cooling conditions, this overload factor can vary during the day as a consequence of variations of ambient temperature, wind flow, and solar radiation.

4.5 An Enhanced Transformer Load Capability Management

As the fig. 6 shows, the hottest-spot and the core temperature do not reach a steady-state value equal to the ambient temperature during the night, although the PV-system is not generating power. This can be explained by the occurrence of no-load losses in the transformer, resulting from the presence of a remanent magnetic flux within the core, which eventually keeps the transformer temperature above the ambient temperature. Additionally, the time window during the night is lower than the time required to reach the thermal steady-state. Figure 10 shows the transformer losses during the time analyzed. The no-load losses (P_C) are constants in contrast to the load losses that depend on the generation (P_E) and the conductor temperature (P_{i^2R}).

A simulation was performed in order to obtain the maximum transformer capability, providing that the transformer is disconnected from the the grid during the nights or during non-radiation hours. Figure 11 shows: the simulated temperature during the analyzed load profile window for both cases (connected and disconnected). The maximum allowed capability obtained without exceeding the transformer design hottest-spot (180 °C) was the same in both cases: 1.95 times. However, disconnecting the transformer during non-generation periods means that the system efficiency is increased. The authors suggest disconnecting the PV-transformer at night in accordance with IEEE Std C57.159™-2016 [7], in order to increase the system efficiency, providing that the PV-inverter does not supply ancillary services.

5 Discussion

The proposed methodology can be used at the transformer design stage, the operation assessment of PV-Transformers, or the expansion planning of PV-Systems. In the course of the design stage, the algorithm can be used during the factory

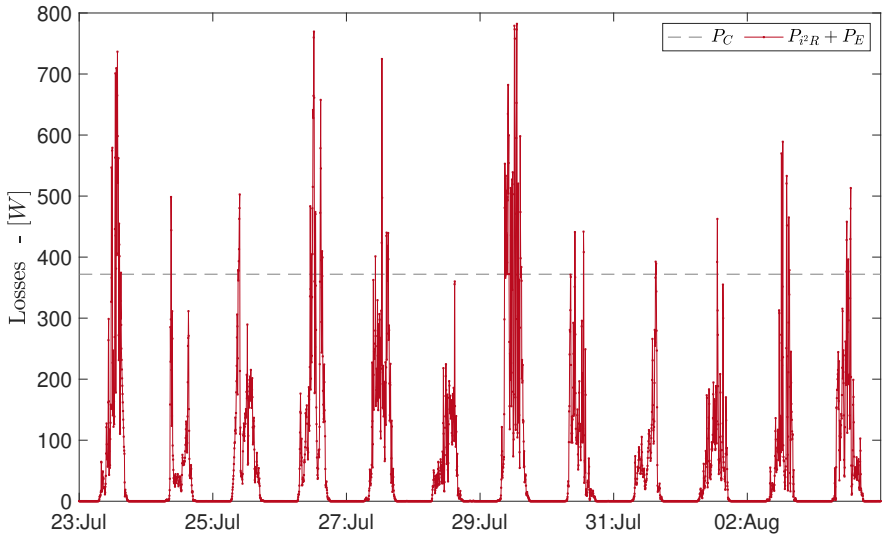

Fig. 10: PV-transformer losses during the time window analyzed

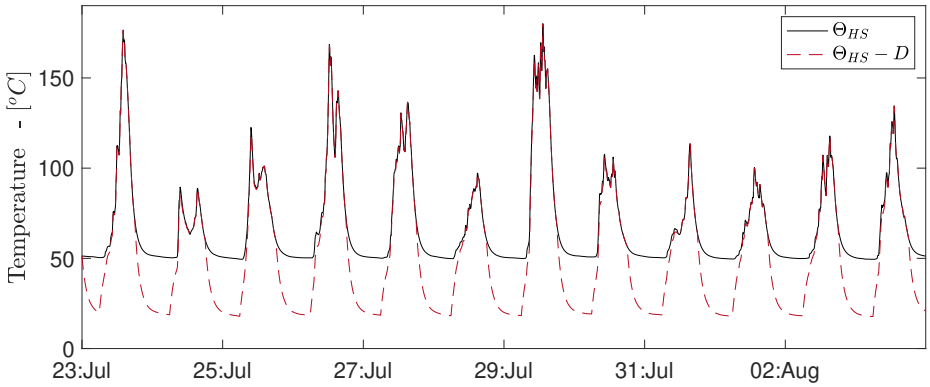

Fig. 11: Maximum transformer overload allowed using the studied PV-generation profile, for the system connected and disconnected to the PV-transformer during no-load generation

load test of a transformer sample in order to obtain the transformer dynamic thermal model under different PV-generation conditions. With this model, the required rated power of the transformer can be estimated, allowing the selection of a more efficient and cheaper transformer. Depending on the PV-generation location, the selection of the transformer rating can be optimized. During operating assessment, the dynamic thermal behavior of the transformer can be modeled by means of real-time measurements and the proposed algorithm, in order to assess overloads and estimate the transformer remaining life. Transformer aging can be estimated using hot-spot temperature and the Arrhenius equation. Finally, amid expansion planning of PV-systems, the historic of both PV-generation and trans-

former temperature can be used to enhance the transformer rating, foreseeing a future expansion.

For small PV installations without temperature nor power monitoring, the thermal performance can be estimated employing the proposed thermal circuit and using historical records, maps or extrapolations of measurements of near areas of both ambient temperature and solar radiation, providing that constants n and m were estimated during factory test.

6 Conclusion

This work addresses a state estimator algorithm, which allows obtaining the load capability of Dry-Type transformers used in PV-systems to connect the inverter to the grid. With this algorithm, both transformer winding and core temperature are estimated in order to compute a dynamic thermal rating.

The algorithm is based on an Extended Kalman Filter and uses the generation cycle of the PV-system, as well as measurements of ambient temperature, windings and core. With this information and the transformer thermal characteristics, the proposed algorithm is implemented in order to fit the parameters of an equivalent thermal circuit. An accurate model of the thermal transient is thus obtained.

According to the results obtained in this work, a dynamic thermal model can be used to assess PV-transformer capability. In this case study, the maximum allowable PV-capability estimated for the 75 kVA Dry-type transformer, without affecting its normal life expectancy, was 140 kW. This capability can vary according to different environmental conditions, for instance locations with different patterns of ambient temperature and solar radiation. Finally, using this algorithm, overloads above the acceptable hottest-spot can be assessed and managed. This is open to future research. In this work, the thermal constants were fitted using data from a tropical zone, where small variations in profiles of both ambient temperature and radiation are expected. Therefore, the algorithm still needs to be validated with temperate conditions.

Conflict of interest

The authors declare that they have no conflict of interest.

Appendix

In order to implement the proposed EKF, the following set of equations were derived, where the subscript , R is related to the rated condition.

$$\frac{d\Theta_{HS}}{dt} = \frac{n\left(P_C + L^2\left(P_{i^2R,R}K_T + \frac{P_{eddy,R}}{K_T}\right) - \frac{\Theta_{HS}-\Theta_a}{R_{0,R}\left(\frac{\rho(\Theta_{HS})}{\rho(\Theta_{HS,R})}\right)^m}\right)}{m_pC_p} \tag{8}$$

$$\frac{df}{d\Theta_{HS}} = \frac{n}{m_pC_p}\left(L^2\left(\frac{P_{i^2R,R}}{T_k+\Theta_{HS,R}} - \frac{P_{eddy,R}}{K_T(T_k+\Theta_{HS})}\right) - \frac{1}{R_{0,R}\left(\frac{\rho(\Theta_{HS})}{\rho(\Theta_{HS,R})}\right)^m} + \frac{m(\Theta_{HS}-\Theta_a)\left(1.07\cdot10^{-5}\Theta_{HS}-3.78\cdot10^{-3}\right)}{\rho(\Theta_{HS})R_{0,R}\left(\frac{\rho(\Theta_{HS})}{\rho(\Theta_{HS,R})}\right)^m}\right) \tag{9}$$

$$\frac{df}{dn} = \frac{P_C + L^2\left(P_{i^2R,R}K_T + \frac{P_{eddy,R}}{K_T}\right) - \frac{\Theta_{HS}-\Theta_a}{R_{0,R}\left(\frac{\rho(\Theta_{HS})}{\rho(\Theta_{HS,R})}\right)^m}}{m_pC_p} \tag{10}$$

$$\frac{df}{dm} = \frac{(\Theta_{HS}-\Theta_a)\,n\ln\left(\frac{\rho(\Theta_{HS})}{\rho(\Theta_{HS,R})}\right)}{R_{0,R}\left(\frac{\rho(\Theta_{HS})}{\rho(\Theta_{HS,R})}\right)^m m_pC_p} \tag{11}$$

$$\frac{df}{dL} = \frac{n2L\left(P_{i^2R,R}K_T + \frac{P_{eddy,R}}{K_T}\right)}{R_{0,R}\left(\frac{\rho(\Theta_{HS})}{\rho(\Theta_{HS,R})}\right)^m m_pC_p} \tag{12}$$

$$\frac{df}{d\Theta_a} = \frac{n}{R_{0,R}\left(\frac{\rho(\Theta_{HS})}{\rho(\Theta_{HS,R})}\right)^m m_pC_p} \tag{13}$$

References

1. Alvarez, D.L., Rivera, S.R., Mombello, E.E.: Transformer Thermal Capacity Estimation and Prediction Using Dynamic Rating Monitoring. IEEE Transactions on Power Delivery **34**(4), 1695–1705 (2019). DOI 10.1109/TPWRD.2019.2918243. URL https://ieeexplore.ieee.org/document/8720053/
2. Alvarez, D.L., da Silva, F.F., Mombello, E.E., Bak, C.L., Rosero, J.A.: Conductor Temperature Estimation and Prediction at Thermal Transient State in Dynamic Line Rating Application. IEEE Transactions on Power Delivery **33**(5), 2236–2245 (2018). DOI 10.1109/TPWRD.2018.2831080. URL https://ieeexplore.ieee.org/document/8352008/

3. Awadallah, M.A., Xu, T., Venkatesh, B., Singh, B.N.: On the Effects of Solar Panels Distribution Transformers. IEEE Transactions on Power Delivery **31**(3), 1176–1185 (2016). DOI 10.1109/TPWRD.2015.2443715. URL http://ieeexplore.ieee.org/document/7127048/
4. Blanco Alonso, P.E., Meana-Fernández, A., Fernández Oro, J.M.: Thermal response and failure mode evaluation of a dry-type transformer. Applied Thermal Engineering **120**, 763–771 (2017). DOI 10.1016/j.applthermaleng.2017.04.007. URL http://linkinghub.elsevier.com/retrieve/pii/S1359431116331210
5. Bracale, A., Caramia, P., Carpinelli, G., De Falco, P.: SmarTrafo: A Probabilistic Predictive Tool for Dynamic Transformer Rating. IEEE Transactions on Power Delivery pp. 1–1 (2020). DOI 10.1109/TPWRD.2020.3012180. URL https://ieeexplore.ieee.org/document/9151393/
6. C57.134™: IEEE Guide for Determination of Hottest-Spot Temperature in Dry-Type Transformers (2013)
7. C57.159™: IEEE Guide on Transformers for Application in Distributed Photovoltaic (DPV) Power Generation Systems (2016)
8. C57.96™: IEEE Guide for Loading Dry-Type Distribution and Power Transformers IEEE Power and (2013)
9. Chen, W., Su, X.: Application of Kalman filter to hot-spot temperature monitoring in oil-immersed power transformer. IEEJ Transactions on Electrical and Electronic Engineering **8**(4), 322–327 (2013). DOI 10.1002/tee.21862. URL http://doi.wiley.com/10.1002/tee.21862
10. Dong, M.: A Data-driven Long-term Dynamic Rating Estimating Method for Power Transformers. IEEE Transactions on Power Delivery pp. 1–1 (2020). DOI 10.1109/tpwrd.2020.2988921. URL https://doi.org/10.1109/TPWRD.2020.2988921https://ieeexplore.ieee.org/document/9072510/
11. Eslamian, M., Vahidi, B., Eslamian, A.: Thermal analysis of cast-resin dry-type transformers. Energy Conversion and Management **52**(7), 2479–2488 (2011). DOI 10.1016/j.enconman.2011.02.006. URL http://linkinghub.elsevier.com/retrieve/pii/S0196890411000781
12. IEEE Std C57.110™-2018 (Revision of IEEE Std C57.110-2008): IEEE Recommended Practice for Establishing Liquid-Immersed and Dry-Type Power and Distribution Transformer Capability When Supplying Nonsinusoidal Load Currents (2018). DOI 10.1109/IEEESTD.2018.8511103
13. Lee, M., Abdullah, H.A., Jofriet, J.C., Patel, D.: Thermal modeling of disc-type winding for ventilated dry-type transformers. Electric Power Systems Research **80**(1), 121–129 (2010). DOI 10.1016/j.epsr.2009.08.007. URL http://linkinghub.elsevier.com/retrieve/pii/S0378779609001989
14. Lu, H., Borbuev, A., Jazebi, S., Hong, T., de León, F.: Smart load management of distribution-class toroidal transformers using a dynamic thermal model. IET Generation, Transmission & Distribution **12**(1), 142–149 (2018). DOI 10.1049/iet-gtd.2017.0360. URL http://digital-library.theiet.org/content/journals/10.1049/iet-gtd.2017.0360
15. Mondol, J.D., Yohanis, Y.G., Norton, B.: Optimal sizing of array and inverter for grid-connected photovoltaic systems. Solar Energy **80**(12), 1517–1539 (2006). DOI 10.1016/j.solener.2006.01.006. URL https://linkinghub.elsevier.com/retrieve/pii/S0038092X06000600
16. Pezeshki, H., Wolfs, P.J., Ledwich, G.: Impact of High PV Penetration on Distribution Transformer Insulation Life. IEEE Transactions on Power Delivery **29**(3), 1212–1220 (2014). DOI 10.1109/TPWRD.2013.2287002. URL http://ieeexplore.ieee.org/document/6675880/
17. Salama, M.M., Mansour, D.E.A., Abdelmakasoud, S.M., Abbas, A.A.: Impact of optimum power factor of PV-controlled inverter on the aging and cost-effectiveness of oil-filled transformer considering long-term characteristics. IET Generation, Transmission & Distribution **13**(16), 3574–3582 (2019). DOI 10.1049/iet-gtd.2019.0409. URL https://digital-library.theiet.org/content/journals/10.1049/iet-gtd.2019.0409
18. Simon, D.: Nonlinear Kalman filtering. In: Optimal State Estimation Kalman, H Infinity, and Nonlinear Approaches, chap. 13, pp. 395–426. John Wiley & Sons, Inc., Hoboken, NJ, USA (2006). DOI 10.1002/0470045345. URL http://doi.wiley.com/10.1002/0470045345
19. Susa, D., Lehtonen, M.: Dynamic thermal modeling of power transformers: Further development - Part I. IEEE Transactions on Power Delivery **21**(4), 1961–1970 (2006). DOI 10.1109/TPWRD.2005.864069. URL http://ieeexplore.ieee.org/document/1705557/

20. Susa, D., Lehtonen, M., Nordman, H.: Dynamic thermal modelling of power transformers. IEEE Transactions on Power Delivery **20**(1), 197–204 (2005). DOI 10.1109/TPWRD.2004.835255. URL http://ieeexplore.ieee.org/document/1375095/
21. Swift, G., Molinski, T., Bray, R., Menzies, R.: A fundamental approach to transformer thermal modeling. II. Field verification. IEEE Transactions on Power Delivery **16**(2), 176–180 (2001). DOI 10.1109/61.915479. URL http://ieeexplore.ieee.org/document/915479/
22. Tellez, S., Alvarez, D., Montano, W., Vargas, C., Cespedes, R., Parra, E., Rosero, J.: National Laboratory of Smart Grids (LAB+i) at the National University of Colombia-Bogota Campus. In: 2014 IEEE PES Transmission & Distribution Conference and Exposition - Latin America (PES T&D-LA), pp. 1–6. IEEE (2014). DOI 10.1109/TDC-LA.2014.6955185. URL http://ieeexplore.ieee.org/document/6955185/
23. Zhang, X., Qian, S., XU, Y., Marek, R., Lei, Q.: Overload Distribution Transformer with Natural Ester and Aramid-Enhanced Cellulose. IEEE Transactions on Power Delivery pp. 1–1 (2020). DOI 10.1109/TPWRD.2020.3015797. URL https://doi.org/10.1109/TPWRD.2020.3015797https://ieeexplore.ieee.org/document/9166742/
24. Zhou, L., Wang, L., Tang, H., Wang, J., Guo, L., Cui, Y.: Oil exponent thermal modelling for traction transformer under multiple overloads. IET Generation, Transmission & Distribution **12**(22), 5982–5989 (2018). DOI 10.1049/iet-gtd.2018.5084. URL https://digital-library.theiet.org/content/journals/10.1049/iet-gtd.2018.5084